Optimization of An O_2-Balanced Bioartificial Pancreas for Type 1 Diabetes Using Statistical Design of Experiment.

Anne Mouré
IECM, USC 1383 INRAE
Sawsen Bekir
IECM, USC 1383 INRAE
Elodie Bacou
IECM, USC 1383 INRAE
Karine Haurogne
IECM, USC 1383 INRAE
Marie Allard
IECM, USC 1383 INRAE
Laurence De Beaurepaire
IECM, USC 1383 INRAE
Steffi Bosch
IECM, USC 1383 INRAE
David Riochet
France SSR Pédiatriques ESEAN-APF, Nantes
Olivier Gauthier
CRIP
Gilles Blancho
CRTI, UMR 1064, INSERM, Université de Nantes
Jean-Paul Soulillou
CRTI, UMR 1064, INSERM, Université de Nantes
Denis Poncelet
GEPEA, UMR CNRS 6144
Grégoire Mignot
IECM, USC 1383 INRAE
Philippe Courcoux
StatSC, USC 1381 INRAE, Oniris
Dominique Jegou
IECM, USC 1383 INRAE
Jean-Marie Bach

IECM, USC 1383 INRAE

Mathilde Mosser (mathilde.mosser@oniris-nantes.fr)

IECM, USC 1383 INRAE

Research Article

Keywords: Optimization, pancreas, diabetes, statistical design, experiment, limitation, supply, efficiency

Posted Date: June 16th, 2021

DOI: https://doi.org/10.21203/rs.3.rs-600404/v1

Version of Record: A version of this preprint was published at Scientific Reports on March 18th, 2022. See the published version at https://doi.org/10.1038/s41598-022-07887-w.

Abstract

A bioArtificial pancreas (BAP) encapsulating high pancreatic islets concentration is a promising alternative for type 1 diabetes. However, the main limitation of this approach is O_2 supply, especially until graft neovascularization. Here, we described a methodology to design an optimal O_2-balanced BAP using statistical design of experiment (DoE). A full factorial DoE was first performed to screen two O_2-technologies on their ability to preserve pseudo-islet viability and function under hypoxia and normoxia. Then, response surface methodology was used to define the optimal O_2-carrier and islet seeding concentrations to maximize the number of viable pseudo-islets in the BAP containing an O_2-generator under hypoxia. Monitoring of viability, function and maturation of neonatal pig islets for 15 days *in vitro* demonstrated the efficiency of the optimal O_2-balanced BAP. The findings should allow the design of a more realistic BAP for humans with high islets concentration by maintaining the O_2 balance in the device.

Introduction

The transplantation of a bioartificial pancreas (BAP), in which pancreatic islets are enclosed and protected in an immuno-isolating biomaterial, is a promising therapy for type 1 diabetes that does not entail strong immunosuppression in patients[1]. The BAP would also overcome the hurdle of human organ shortage by allowing the use of alternative islet sources. In particular, neonatal pig islets (NPIs) seem very promising because their isolation process is easily transposable to a clinical application in terms of good manufacturing practices and the stability of the phenotype of these primary cells[2]. However, one of the main limitations to the clinical success of BAP is the limited O_2 supply to the encapsulated islet cells[3–5]. The O_2 balance in the BAP results from complex interactions between several parameters including O_2 consumption by the encapsulated cells, O_2 diffusivity through the encapsulating material, geometrical features of the device, local O_2 partial pressure (pO_2) at the transplantation site, and vascularization of the graft surface[6].

Pancreatic islets are large cell clusters that consume high amounts of O_2[7] and are very sensitive to hypoxia[8]. In the pancreas, a partial O_2 pressure (pO_2) of 40 mmHg (5%) has been reported in the endocrine tissue[9]. The *in situ* pO_2 value should even be higher in pancreatic islets directly perfused with O_2-rich arterial blood (80–100 mmHg) through a dense capillary network. During the isolation process, islets lose their vasculature, and the immuno-isolating membrane of the BAP prevents direct revascularization of the cell clusters. As a consequence, cell survival only relies on the passive diffusion of O_2 through the BAP capsule and the cell clusters. After islets transplantation, the O_2 tension in the environment surrounding the graft is assumed to be approximately 40 mmHg in extravascular sites[4,10–12]. Before graft surface neovascularization takes place within the first 2 weeks, O_2 tensions may be below 5 mmHg (< 1%), even in naked islet grafts[9,13]. Pancreatic islet culture under low O_2 tension results in impaired insulin secretion when pO_2 of the media is < 50 mmHg[12,14] and islet cell death when

pO_2 is < 5 mmHg[4,12]. Furthermore, dying cells release molecules and signals that could trigger an unwanted pro-inflammatory response, likely contributing to early graft failure[15–17].

BAP capsules can be categorized into microcapsules and macrocapsules based on their size. Although spherical microcapsules seem the most suitable geometry from the standpoint of O_2 diffusion, macrocapsules have a major advantage in terms of safety, as they can be fully retrieved and replaced. Theoretical modeling has been used to predict O_2 distribution and hypoxic regions in BAPs according to the device's geometry, islet size and density, surrounding O_2 tension, and O_2 diffusion across encapsulating materials[4,6,12,18]. Several studies aimed to optimize the features of BAPs to achieve therapeutic efficiency and avoid hypoxia-induced damages[4,12]. It is estimated that approximately 10,000 islet equivalent (IEQ)/kg in the body are needed to restore normoglycemia in type 1 diabetes patients[5,19], even considering a high pO_2 of 40 mmHg outside the device. This requires large devices of 27 to 150 m for hollow fibers[4,12] or 211 to 600 cm^2 for planar devices depending on their width[4,5,12]. These dimensions are not amenable for human clinical transplantation. Pancreatic islets need thus to be encapsulated at a higher density in the BAP to obtain a device size that is suitable for clinical application[5]. However, increasing islet density in the device further decreases the O_2 availability in the BAP. Thus, designing strategies to improve the O_2 supply is necessary[4,15,17].

Many strategies have been developed to address O_2 limitations in the BAP. They include use of hypoxia-resistant cells[20], increased vascularization induction around the device[11,21,22], increased O_2 diffusivity through the encapsulating biomaterial [23,24], and an exogenous O_2 source[24–27]. One of the most promising strategies uses a gas delivery system developed by Beta O_2 Technologies (Rosh-Haayin, Israel). In this system, O_2 enriched gas is injected into the Beta air device to deliver O_2 to islets that are macro-encapsulated in alginate through a diffusion membrane. This BAP can maintain normoglycemia for 7 months in diabetic rats and should enable a therapeutically efficient device of 100 cm^2 in type 1 diabetic patients. However, this strategy requires daily O_2 injections[28].

We recently described the potential of a combination of utilization of the extracellular hemoglobin HEMOXCell with an implantable O_2 generator composed of silicone-encapsulated calcium peroxide, to supply O_2 to alginate macro-encapsulated NPIs up to 7 days in a hypoxic environment[24]. Nevertheless, an optimization step aiming to fine-tune the O_2 balance between a high islet density and the O_2 supply capacity of the oxygenation strategy remains crucial to design a functional BAP to treat type 1 diabetes. The aim of the present study was to optimize the configuration of the BAP incorporating the O_2 strategy by using a Design of Experiments (DoE) approach, including factorial design and response surface methodology (RSM). These statistical tools methods provide efficient ways to understand the complex relationships between input factors and output responses in a biological system, including the interactions between factors[29]. Using the DoE methodology, we aimed to i) validate the efficiency of the oxygenation strategy on alginate encapsulated MIN6 beta cell pseudo-islets, (ii) design an optimal O_2-

regulated BAP with high islet density carrying the oxygenation strategy, and (iii) assess the optimal BAP design on NPI viability, function, maturation, and hypoxic stress *in vitro*.

Methods

The study was carried out in compliance with the ARRIVE guidelines.

Animals and ethical concerns. The data were the collective results gathered from eight neonate pigs. Mini pigs aged 2 to 12 days were obtained from the INRAE PEGASE unit (Rennes, France). Experiments using pigs were approved by the Pays de la Loire Ethic Committee (Approval 01074.01/02) and were carried out in accordance with the relevant French (2013 – 118) and European regulations (2010/63 EU Directive). All efforts were made to minimize animal suffering and to restrict the number of experimental animals. Analgesia and anesthesia were provided by IM injection of methadone, midazolam and ketamine, and maintained with 2% isofluran. Piglets were subjected to laparotomy, and the pancreas was removed after exsanguination via the aorta causing euthanasia.

Pancreatic islet isolation. NPIs were isolated from mini-pig pancreas as described previously[57]. Briefly, the pancreas was cut into 1 to 2 mm^3 small pieces and digested with 25 mg/mL collagenase type V-S (Sigma-Aldrich, Saint-Louis, MO, USA) with gentle agitation for 14 to 16 min at 37°C. The digest was filtered through a 500 µm pore size filter, washed in HBSS buffer supplemented with 0.5% (w/w) bovine serum albumin (BSA, Sigma-Aldrich), and then cultured in Ham's F10 (Dutscher, Brumath, France) supplemented with 10 mM glucose, 50 mM IBMX, 2 mM L-glutamine, 10 mM nicotinamide, 100 IU/mL penicillin, and 100 mg/mL streptomycin. NPIs were cultured for at least 24 h in a normoxic condition (37°C, 20% O_2, 5% CO_2) before encapsulation into alginate sheets.

Pseudo-islet formation. The mouse MIN6 beta cell line was kindly provided by Pr. Jun-ichi Miyazaki (Osaka University Medical School, Japan)[58]. MIN6 cells were expanded in DMEM medium (Dutscher, Brumath, France) supplemented with 10% heat-inactivated calf serum (Invitrogen, Villebon-sur-Yvette, France), 1% penicillin/streptomycin / neomycin, and 50 µM 2-mercaptoethanol. To generate MIN6 pseudo-islets (MPIs), 10^6 MIN6 cells/mL were cultured in non-treated culture petri dishes for 3 days at 37°C in an atmosphere of 20% O_2 and 5% CO_2.

Alginate encapsulation. Clinical grade low viscosity and high guluronate sodium alginate 2.2% (w/v) (PRONOVA UP LVG, Novamatrix, Sandvika, UK) was used for islet (NPIs and MPIs) encapsulation. Alginate was solubilized in 0.9% NaCl (w/v) by gentle stirring overnight at 4°C and sterilized using 0.2 µm filtration. NPIs and MPIs were quantified using canonical standardized Islets Equivalent Quantities (IEQ)[59]. For encapsulation in alginate macrobeads, islets were gently mixed in the hydrogel at 2 500 IEQ/mL alginate. Macrobeads 3 mm in diameter were obtained by alginate extrusion through a 23 G needle using a syringe driver into a 100 mM $CaCl_2$ gelation bath for 5 min. Alginate sheets (680 µm thickness, 1.2 cm diameter) containing varying islet concentrations (2,000 to 46,667 IEQ/mL alginate) were prepared in 48-well plate (P48) lids by pouring 75 µL of the alginate suspension on the well surface

on the lid. Crosslinking of flat alginate sheets was achieved by covering the lid wells with 0.22 µm filters (Merck Millipore, Burlington, MA, USA) associated with sintered glass filters (DWK Life Sciences, Wertheim, Germany) previously soaked in a 100 mM $CaCl_2$ solution. A volume of 5 mL of $CaCl_2$ solution was added to the top of the glass filter before a 7 min incubation at room temperature. After crosslinking, alginate beads or sheets were washed twice in 0.9% NaCl and then in NPI or MPI culture medium.

Encapsulated islet culture. Eight macrobeads were placed in each P48-well plate well containing 500 µL of culture medium. Alginate sheets were cultured in 12-well plate inserts in 3 mL of culture medium (two sheets per insert) or in 24-well plates in 1.5 mL of medium (one sheet per well). Encapsulated islets were incubated either in a normoxic O_2 tension environment (20% O_2, 5% CO_2, 37°C) or in a hypoxia chamber (STEMCELL Technologies, Grenoble, France) filled with 1% O_2 and 5% CO_2 in N_2 (37°C), mimicking the O_2 tension encountered after transplantation. Culture media were renewed every 2 to 3 days of culture.

Pseudo-islet viability assessment. Viable cell content in encapsulated islets was determined by intracellular ATP quantification (RLU, relative light unit) using the CellTiter-Glo® 3D Cell Viability kit (Promega, Charbonnieres-les-Bains, France) following the manufacturer's recommendations. The ATP content standard curve for MPIs was obtained from pseudo-islets immediately after encapsulation in alginate patches at several densities. A linear correlation was observed between the luminescent signal of the CellTiter-Glo® 3D Cell Assay and the fluorescent Cyquant DNA Assay regardless of the culture conditions (data not shown). Cell death within the encapsulated islets was evaluated by quantifying the lactate dehydrogenase activity (LDH, absorbance unit (AU), Roche, Meylan, France) in culture supernatants according to the manufacturer's recommendations. ATP luminescence and LDH absorbance were evaluated on a FLUOstar OPTIMA luminometer (BMG Labtech, Champigny-sur-Marne, France).

Insulin secretion assay. The capacity of encapsulated islets to secrete insulin following metabolic stimulation was evaluated by 30 min sequential incubations of alginate encapsulated islets in basal medium (RPMI [PAA, Velizy-Villacoublay, France] containing 2 mM L-glutamine, 0.5% BSA, and 2.8 mM glucose), stimulation medium (basal medium supplemented with 20 mM glucose and 10 mM theophylline), and basal medium. Insulin concentrations were assessed in culture supernatants by ELISA (Mercodia). Insulin secretion stimulation indexes were calculated as the ratio of the glucose + theophylline-stimulated insulin secretion level over the basal level of the encapsulated islets.

Intracellular insulin content. NPIs were recovered from the alginate sheet by incubation for 20 min at 37°C in a decapsulating solution (5 mM citrate and 1 mM EDTA in PBS) followed by mechanical dissociation and centrifugation. Proteins from naked or decapsulated NPIs were extracted by repeated pipetting and incubation steps at -20°C in 50 µL of an ethanol-HCL solution. Protein extracts were neutralized by adding 25 µL of Tris-HCL 1M (pH = 7.5). Pig intracellular insulin was assayed in protein extracts by ELISA (Mercodia). Absorbance was evaluated using a FLUOstar OPTIMA luminometer.

Vascular endothelial growth factor (VEGF) quantification. VEGF secretion was assayed by ELISA in islet culture supernatants (Clinisciences, Nanterre, France).

Transcriptomic analysis. Islets were recovered from alginate sheets as previously described and frozen at − 80°C in NucleoZOL reagent (Macherey-Nagel, Düren, Germany). Total RNA was isolated according to the manufacturer's instructions and reverse transcribed using MLV reverse transcriptase (Invitrogen, Carlsbad, CA, USA). Real-time quantitative polymerase chain reaction (RT-qPCR) was performed on a CFX 96 Touch instrument (BioRad, Hercules, CA, USA) using Hot FirePol EvaGreen mix (Solis Biodyne, Tartu, Estonia). The expression of genes encoding RPL19 (ribosomal protein L19) and PPIA (peptidylprolyl isomerase A) were used to standardize the expression of PDX1 (pancreatic and duodenal homeobox 1) and HO1 (heme oxygenase 1). The pig primers used for RT-qPCR are listed in Table 7. For each sample, the relative quantity was extrapolated from a standard curve created through the amplification of serial dilutions of an RNA mix, and extracted from islets cultured under normoxic and hypoxic conditions. The gene expression of this mix was artificially increased by spiking 5 µL of amplification product sequences diluted 1:1250.

Table 7
RT-qPCR primer sequences

Target	Forward	Reverse
RPL19	AACTCCCGTCAGCAGATCC	AGTACCCTTCCGCTTACCG
PPIA	CACAAACGGTTCCCAGTTTT	TGTCCACAGTCAGCAATGGT
PDX1	AAGTCTACCAAGGCTCACGC	CTTGTTCTCCTCGGGCTCTG
HO1	GCTGACCCAGGACACTAAGG	GGAGAGGACGCTGAGCTG

Immunohistological analyses

Slide preparation. NPIs were recovered from alginate sheets as previously described, centrifuged, and fixed in paraformaldehyde (PFA; 4% (v/v)) for 30 min before being embedded in HistoGel™ (Thermo Fisher Scientific, Waltham, MA, USA). Morphology of formalin-fixed paraffin-embedded (FFPE) NPIs in cross-sections (3 µm) were analyzed using Hematoxylin-Eosin-Saffron stain.

Insulin and glucagon immunostaining FFPE cross-sections of NPIs (3 µm) were incubated overnight with rabbit anti-insulin at 1:400 dilution (C27C9; Cell Signaling Technology, Beverly, MA, USA) and mouse anti-glucagon at 1:500 dilution (G2654; Sigma-Aldrich) IgGs, followed by 1 h with secondary Alexa-Fluor 488 donkey anti-rabbit IgG at 1:2000 dilution and Alexa-Fluor 555 donkey anti-mouse IgG at 1:1000 dilution (Thermo Fisher Scientific).

PDX-1 immunostaining. Slides were incubated overnight with horseradish peroxidase-conjugated anti-PDX-1 antibody at :500 dilution (219207-Abcam, Cambridge, UK). PDX-1 was visualized using EnVision+System-HRP, rabbit (DAB+) (K4011; Agilent, Santa Clara, CA, USA) and counterstained with

hematoxylin. Neonate-pig-pancreatic sections were used as positive controls. Analyses without primary antibodies were performed as a negative control.

Insulin and glucagon quantification Images were acquired using an AxioVert microscope and Zen lite software (Carl Zeiss, Jena, Germany). Photos of representative fields of the slices were taken under both white light and fluorescence using the same exposure time for all images taken with the same staining. The percentage of insulin and glucagon staining per NPI area was quantified using ImageJ software (NIH, Bethesda, MD, USA).

Pseudo-islet O_2 consumption rate The O_2 consumption rate (OCR) by MPIs was measured in bioreactor experiments. OCR was determined on the first day of culture by placing 1,000 IEQ MPIs in a P48 non-treated culture dish in 500 µL of culture medium. Dissolved O_2 concentration was added to the medium with a Clark electrode (InPro 6850i, Mettler-Toledo, Viroflay, France) inserted in the P48 plate wells and the Rhapsody software (Pierre Guerin Technologies, Niort, France). MPI OCR (pmol/min.IEQ) was calculated as the initial slope of the dissolved O_2 concentration curve in the medium. A negative control without islets was performed in parallel.

O_2 supply strategies. The O_2 carrier HEMOXCell hemoglobin (Hemarina, Morlaix, France) was mixed with the pseudo-islets in the alginate before crosslinking into macrobeads or sheets. The O_2-generating biomaterial was prepared by mixing calcium peroxide (Sigma-Aldrich) in polydimethylsiloxane (silicone, Sylgard® 184, Sigma-Aldrich) in a 1:3 ratio (weight/weight) as previously described by Pedraza[27]. A volume of 100 µL per well of silicone-CaO_2 was degassed and cross-linked in a P48 plate for 24 h at 60°C.

Silicone-CaO_2 O_2 production rate The O_2 production rate (OTR) of the silicone-CaO_2 disks was followed during culture for 12 days by placing four silicone-CaO_2 disks in 200 mL of PBS (Eurobio, Courtaboeuf, France) at 37°C. The PBS was first deoxygenated by stirring at 200 rpm in a hypoxic atmosphere (N_2). After reaching 0% O_2, the container was sealed and the dissolved O_2 concentration was measured in the PBS using a Clark electrode and Rhapsody software. OTR (nmol/min/disk) was calculated as the initial slope of the dissolved O_2 concentration curve in the PBS. A negative control without a silicone-CaO_2 disk was performed in parallel.

DoE.

Screening Screening of the oxygenation strategies was performed on MPIs encapsulated in alginate macrobeads using a full factorial design 2^3 (Figure 1). The influence of the main factors and their first-order interactions was analyzed. The three factors studied and their levels were: without/ with HEMOXCell, without/ with silicone-CaO_2 and normoxic/hypoxic O_2 tension. The response variables were intracellular ATP content per well (RLU), ATP/LDH viability ratio per well (RLU/AU), and insulin stimulation index. These response variables were assessed after 6 days of culture under the different conditions defined by the experimental design (Table 2).

RSM Based on the screening of the O_2 strategies, RSM was used to optimize the BAP configuration concerning the O_2 balance in the alginate sheet device. The objective was to maximize the density of viable MPIs in the BAP by tuning the HEMOXCell concentration and the islet seeding density in the hypoxic environment in the presence of the silicone-CaO_2 disk. A central composite design (2^2 factorial design with 4-star points and four replicates of the central point) was used to fit a second-order polynomial model (Figure 3C). The model validation was performed by analyzing the lack-of-fit test results, the determination coefficient R^2 value, and the diagnostic plots. The two factors studied were HEMOXCell concentration and islet seeding density, and their ranges were determined according to the literature and the determination of silicone-CaO_2 OTR and pseudo-islet OCR. The response variables were intracellular ATP content (RLU) and ATP/LDH viability ratio (RLU/AU) per device. These response variables were assessed on pseudo-islets encapsulated in alginate sheets cultured for 24 h under the different conditions defined by the experimental plan (Table 5). The optimum values were determined by solving the regression equations and analyzing the response surface plots. A multi-response optimization was performed to achieve the best compromise to maximize viability and function of the encapsulated pseudo-islets.

Statistical analyses. The experimental design for the screening and the optimization steps were repeated independently at least three times. Analysis of variance (ANOVA), regression analysis, and graphical display of DoE results were performed using the Statgraphics Centurion software 18.1.06. Assessment of the optimal BAP design on NPIs was performed on a minimum of four independent experiments. The significance of differences between groups was evaluated using a non-parametric test (Mann-Whitney or paired Wilcoxon tests) or a parametric unpaired t-test. A p-value <0.05 was considered statistically significant.

Results

Screening of O_2 supply strategies for BAP containing MIN6 pseudo-islets (MPIs). The first objective of this study was to screen the selected O_2 strategies (HEMOXCell and silicone-CaO_2) in two different O_2 tension environments (normoxia and hypoxia) for their impact on the viability and function of encapsulated MPIs using a 2^3 screening experimental design after 6 days of culture (Fig. 1A). The DoE was analyzed using variance analysis (Suppl. Tables 1 to 3). The models seemed to adjust well to the experimental data with determination coefficients (percentage of total variations explained by the model, R^2) higher than 0.80 (Suppl. Table 1 to 3). The experimental data obtained (Table 1) revealed the benefit of the presence of HEMOXCell on pseudo-islet viability, with a significant positive effect of this factor on the ATP content ($p < 0.05$, Table 2). The positive effects of the silicone-CaO_2 disk on the ATP content and the ATP/ LDH viability ratio were more evident ($p < 0.001$, Table 2), with a trend for better on the insulin stimulation index ($p = 0.0633$, Table 2). As expected, the hypoxic environment had a strong negative impact on pseudo-islet viability and function, with significant effects of O_2 tension on ATP content, ATP/ LDH ratio, and insulin index ($p < 0.01$, Table 2). A significant interaction was evident between silicone-

CaO_2 and the O_2 tension (BC) on the ATP content ($p < 0.001$, Table 2). A strong positive effect of silicone-CaO_2 on the MPI ATP content was observed in the hypoxic environment, while a negative effect of this factor was observed under normoxic conditions (Fig. 1B, interaction BC). Interestingly, a significant positive interaction was evident between HEMOXCell and silicone-CaO_2 (AB) on the ATP content ($p < 0.05$, Table 2), as was a benefit on the ATP/ LDH viability ratio ($p = 0.0890$, Table 2). The effect of HEMOXCell was higher in combination with silicone-CaO_2 than alone and vice-versa for these two responses (Fig. 1B). Even if not significant, we also observed a positive interaction between HEMOXCell and the O_2 tension on the insulin stimulation index, with a higher effect of HEMOXCell in the normoxic environment. A multi-response optimization was performed to find the best condition to maximize pseudo-islet viability and function in the BAP in the hypoxic environment (Table 3). The best conditions under hypoxia were found in the presence of HEMOXCell and silicone-CaO_2. These optimal conditions resulted in an increase of ATP content and ATP/LDH viability ratio by 14% and 48% respectively, while a decrease of insulin stimulation index by 19% was observed compared to the normoxic control without the O_2 strategy (Table 1).

Table 1
Factorial design matrix and experimental results obtained for the screening DoE.

Run	Factors			Responses *		
	Factor A HEMOXCell	Factor B Silicone-CaO_2	Factor C O_2 tension	ATP content ($x10^6$ RLU)	ATP/ LDH ratio ($x10^6$ RLU/AU)	Insulin stimulation index
1	Without	Without	Normoxia	13.52	9.66	3.1
2	With	Without	Normoxia	13.45	7.78	3.1
3	Without	With	Normoxia	9.09	14.26	3.1
4	With	With	Normoxia	13.43	21.47	4.5
5	Without	Without	Hypoxia	6.11	5.12	1.7
6	With	Without	Hypoxia	6.13	4.94	1.3
7	Without	With	Hypoxia	13.98	13.28	2.2
8	With	With	Hypoxia	15.41	14.28	2.5

*Mean of three independent experiments

Table 2
Estimated effects of factors and interactions and their statistical significance in the screening DoE.

Factors	ATP content ($\times 10^6$ RLU)		ATP/LDH ratio ($\times 10^6$ RLU/ AU)		Insulin stimulation index	
	Estimated effect ± SD	p-value *	Estimated effect ± SD	p-value *	Estimated effect ± SD	p-value *
A HEMOXCell	**1.68 ± 0.57**	**0.0109**	1.52 ± 1.39	0.2928	0.38 ± 0.36	0.3160
B Silicone-CaO_2	**2.92 ± 0.57**	**0.0002**	**8.97 ± 1.39**	**0.0000**	0.81 ± 0.39	0.0633
C O_2 tension	**2.05 ± 0.55**	**0.0027**	**4.11 ± 1.35**	**0.0095**	**1.61 ± 0.36**	**0.0013**
AB interaction	**1.71 ± 0.57**	**0.0100**	2.55 ± 1.39	0.0890	0.45 ± 0.36	0.2404
AC interaction	0.63 ± 0.55	0.2788	0.91 ± 1.35	0.5152	0.45 ± 0.36	0.2380
BC interaction	**-5.32 ± 0.55**	**0.0000**	0.42 ± 1.35	0.7630	-0.15 ± 0.36	0.6838

*p-values are computed from the analysis of variance performed for each response (Suppl. Tables 1 to 3). Statistical significance at 10% and 5% are highlighted in blue and **bold**, respectively.

Table 3
Multi-response optimization for the screening DoE

Optimization	Optimal level of factors			Response values at the optimum		
	Factor A HEMOXCell	Factor B Silicone-CaO_2	Factor C O_2 tension	ATP content ($x10^6$ RLU)	ATP/LDH ratio ($x10^6$ RLU/AU)	Insulin stimulation index
Optimization in hypoxia	with	with	hypoxia	15.74	15.16	2.6

Optimization of the BAP design concerning O_2 balance. In the second part of the study, the objective was to optimize the configuration of the BAP carrying the previously defined O_2 strategy in a hypoxic environment to increase the density of viable islets in the device. To incorporate the O_2 strategy, the BAP was made of two sheets of alginate encapsulating islets and HEMOXCell. The sheets were placed on either side of the silicone-CaO_2 disk. A central composite experiment was designed to maximize the density of viable islets in the BAP (ATP content and ATP/LDH ratio) by tuning the HEMOXCell concentration and the islet seeding density (Fig. 2C). As primary islets used in the BAP in clinical settings would not proliferate, we optimized the device configuration on MPIs over a short (24 h) period, where

differences in MIN6 cell proliferation were negligible (Suppl. Figure 1). A HEMOXCell concentration ranging from 50 to 500 µg/mL was defined according to the literature[24,30,31]. The islet seeding density range was chosen on the basis of the O_2 balance in the BAP. One silicone-CaO_2 was able to produce a mean of 11.9 ± 0.3 nmol/min of O_2 over 12 days (Fig. 2A). MPI OCR was estimated to be 1.04 ± 0.48 pmol/min.IEQ (Fig. 2B), giving a maximal islet density of 11,500 IEQ that could be supplied with O_2 per silicone-CaO_2 disk. In the literature, OCR was typically found to be approximately 1.64 ± 0.36 pmol/min.IEQ for human pancreatic islets[28,32–35] and 2.2 ± 0.42 pmol/min.IEQ for neonate pig islets[33,36], suggesting a maximal islet density of 7,300 and 5,400 per silicone-CaO_2 disk, respectively. Based on these estimations, we decided to evaluate the islet seeding density range of 300 to 7,000 IEQ in the BAP device (Table 4).

The optimization DoE was analyzed using variance analysis (Suppl. Tables 4 and 5). The resulting models adjusted well to the experimental data concerning ATP content according to the high R^2 value obtained (0.76, n = 6). In contrast, a low R^2 value was observed for the ATP/LDH ratio (0.39, n = 5), suggesting that factors other than those tested are involved in the response variations observed. Nevertheless, the lack-of-fit tests remained non-significant for both ATP content and ATP/ LDH ratio (Suppl. Tables 4 and 5). The analysis of diagnostic plots confirmed the aforementioned results concerning model validation with overall good prediction for the ATP content, while poorer results were obtained for the ATP/LDH ratio (Suppl. Figure 2). This was consistent with the higher experimental variability for the ATP/LDH ratio of the raw data obtained (Suppl. Figure 2).

The application of RSM resulted in the following regression equation, modeling the relationship between the response variables and the factors as a second-order polynomial function:

$$Y = \beta_0 + \beta_A X_A + \beta_B X_B + \beta_{AB} X_A X_B + \beta_{AA} X_A^2 + \beta_{BB} X_B^2 + \varepsilon$$

where Y is the response; X_A and X_B are the linear variables associated with factors A and B, X_A^2 and X_B^2 the quadratic variables associated with factors A and B, β the coefficient associated with these variables, and ε is the residual variation. Estimates of regression coefficients and response surfaces are presented for each biological parameter tested in Suppl. Table 6 and Fig. 2D and 2E. We observed a significant quadratic effect of HEMOXCell concentration (AA) on ATP content ($p < 0.05$, Table 5). As expected, a strong positive effect of the islet seeding density on ATP content was observed ($p < 0.0001$, Table 5). Moreover, a negative quadratic effect of the islet seeding density (BB) was also observed for this parameter ($p < 0.01$, Table 5). No significant interaction was observed between the HEMOXCell concentration and the islet seeding density in the device.

According to these data, increasing the islet seeding density increased the viable cell content in the BAP but reached a plateau for the higher densities tested (Fig. 2D). Moreover, high islet density also resulted in a decreased islet viability ratio in the device (Fig. 2E). Multi-response optimization was used to determine the optimal HEMOXCell concentration and islet seeding density to maximize the ATP content and the

ATP/ LDH ratio in the BAP (Table 6). To this end, a desirability function was defined to find the best compromise between the two response variables. The optimal BAP configuration was defined as 50 µg/mL of HEMOXCell and 3,284 IEQ/device in the presence of the silicone-CaO_2 disk in a hypoxic environment. According to the standard curves of ATP content from viable encapsulated MPIs, we estimated the corresponding number of viable islets in the optimized BAP (Suppl. Figure 3). An estimated cell number equivalent to 3,572 IEQ was viable after 24 h in the hypoxic environment with the O_2 strategy. As a comparison, the multi-response optimization was also performed with data obtained from the same DoE performed in hypoxia without the silicone-CaO_2 disk (Table 6). The analysis of the central composite experimental design without silicone-CaO_2 was carried out in the same way as with the O_2 generator (data not shown). In the absence of the O_2 generator, the optimal BAP configuration was defined with the 500 µg/mL HEMOXCell and 375 IEQ/device (Table 6).

Table 4
Factorial design matrix and experimental results obtained for the optimization DoE.

Run	Factors		Responses*	
	Factor A Islet seeding density (IEQ/device)	Factor B HEMOXCell concentration (µg/mL)	ATP content ($\times 10^6$ RLU)	ATP/ LDH ratio ($\times 10^6$ RLU/AU)
1	1274	115	5.69	12.70
2	1274	435	5.75	8.35
3	6026	115	10.05	3.32
4	6026	435	10.93	4.82
5	300	275	0.87	5.41
6	3625	50	8.60	9.40
7	3625	500	9.60	8.38
8	7000	275	11.16	4.48
9 (central point)	3625	275	8.11	11.86
10 (central point)	3625	275	7.93	9.58
11 (central point)	3625	275	8.12	11.93
12 (central point)	3625	275	6.42	5.31

***** Mean of five independent experiments

Table 5
Estimated effects of factors and interactions and their statistical significance in the optimization DoE (with silicone-CaO_2)

Factors	ATP content (× 10^6 RLU)		ATP/ LDH ratio (× 10^6 RLU/AU)	
	Estimated effect ± SD	p-value*	Estimated effect ± SD	p-value*
A HEMOXCell concentration	4.9 ± 7.63	0.5238	-1.37 ± 2.49	0.5859
B Islet seeding density	**8.34 ± 7.64**	**0.0000**	5.41 ± 2.72	0.0537
AA	2.89 ± 1.30	0.0307	-2.14 ± 4.27	0.6193
BB	**-3.49 ± 1.3**	**0.0098**	-7.65 ± 4.39	0.0893
AB interaction	1.64 ± 1.51	0.9142	6.22 ± 5.12	0.2310

*p-values are computed from the analysis of variance performed for each response (Suppl. Tables 4 and 5) and statistical significance at 10% and 5% are highlighted in blue and **bold**, respectively.

Table 6
Multi-response BAP optimization under hypoxia with and without O_2 strategy

Optimization	Optimal level of factors		Response values at the optimum	
	Factor A HEMOXCell conc.	Factor B Islet density	ATP content per device (RLU)	ATP/LDH ratio (RLU/AU)
With O_2-strategy	50 µg/mL	3,284 IEQ/device	8.73 x 10^6 ≈ 3,572 viable IEQ*	9.64 x 10^6
Without O_2-strategy	500 µg/mL	375 IEQ/device	2.24 x 10^6 ≈ 656 viable IEQ*	3.83 x 10^6

* Number of equivalent viable and dead MPIs interpolated from the ATP content standard curve

(Suppl. Figure 3)

Validation of O_2 balanced BAP design in NPIs Finally, the optimal BAP configuration was validated *in vitro* on primary NPIs in a hypoxic environment mimicking the acute hypoxic period (1% O_2) before graft neovascularization for 15 days. We set the density of NPIs in the BAP to 3,000 IEQ according to the RSM optimization and we chose a HEMOXCell concentration of 500 µg/mL. The results were compared to macro-encapsulated NPIs cultured without the O_2 strategy in hypoxia (negative control) or under high O_2 tension (normoxia, positive control).

As expected, adverse effects of hypoxia without the O_2 strategy on the NPI ATP content were observed compared to the high O_2 tension condition on the different days of analysis (Fig. 3A). Indeed, while the total metabolic activity of NPIs under high O_2 tension was almost completely maintained during the 15 days of culture, it decreased under hypoxia by 15% ($p < 0.05$), 37% ($p < 0.05$), and 63% ($p = 0.0625$) after 3, 8, and 15 days, respectively. Interestingly, in the case of the O_2 balanced BAP, the O_2 strategy significantly increased the ATP content of NPIs on day 3 ($p < 0.05$) and 8 ($p < 0.01$) compared to NPIs cultured without the O_2 strategy (Fig. 3B). This allowed the ATP content to reach that observed in the positive control (Fig. 3A). After 15 days, the O_2 strategy still seemed to improve the NPI ATP content as a 25% increase was observed compared to NPI cultures in hypoxia without the O_2 strategy ($p = 0.1167$). However, at this time, a drop of up to 40% ATP was observed compared to the NPIs cultured under high O_2 tension. The viability (ATP/LDH ratio) of NPIs followed the same trends as observed for the total metabolic activity of NPIs under different conditions (Fig. 3C). Hypoxia decreased the viability of NPIs and the O_2-strategy seemed to improve the viability. However, due to the high variability of LDH levels encountered in cultures, differences between groups were not found significant (Fig. 3D). The effect of O_2 tension on NPI morphology was characterized using hematoxylin and eosin immunohistochemical staining after 9 days of culture (Fig. 3E). NPIs under hypoxia showed altered nuclei, while islets grown under hypoxia with the O_2 strategy had a similar morphology to those cultured under normoxia.

Insulin secretion by the alginate encapsulated NPIs was assessed following glucose plus theophylline (G + T) stimulation after 3, 8, and 15 days of culture (Fig. 4). From day 3 of culture in hypoxia, the NPIs lost their ability to secrete insulin in response to G + T. In high O_2 tension, NPIs remained functional until day 15. In the O_2 balanced BAP, the adverse effect of hypoxia on the insulin-secretory function of NPIs seemed to be highly mitigated, although it failed in some experiments for which lower insulin responses were observed, even in NPIs cultured under high O_2 tension (Fig. 4A, 4B, and 4C). At any day of culture, a significant adverse effect was evident for NPI insulin stimulation indexes triggered by hypoxia from 13.5 ± 5.0 to 1.6±0.4($p<0.005$). This was significantly reversed by the addition of the O_2-strategy to 7.2±2.5 ($p<0.05$) (Fig. 4D). The optimized O_2 strategy attained an NPI stimulation index that was not significantly different ($p=0.262$) from the NPIs cultured under high O_2 tension.

The effect of O_2 tension on NPI maturation was assessed by the quantification of the expression of insulin, glucagon, and PDX-1 after 9 or 15 days of culture compared to day 1 (Fig. 5 and Suppl. Figure 4). The intracellular insulin/ATP ratio of NPIs cultured under high O_2 tension seemed to increase after 15 days, with an increase of 177 ± 37%, while hypoxia prevented this increase (Fig. 5A). The percentage of insulin-stained area in NPIs significantly increased from day 1 to day 8 regardless of O_2 tension ($p < 0.0001$), although the observed increase was lower in hypoxia compared to normoxia ($p < 0.01$, Fig. 5C and 5D). For both conditions, similar trends were observed in PDX-1 mRNA relative expression of NPIs (Fig. 5B) and the percentage of PDX1 positive cells (Suppl. Figure 4). The O_2 strategy seemed to mitigate the hypoxic effect observed on PDX-1 expression, which was similar to the positive control (Fig. 5B). In addition, beta cell maturation increased as shown by the enlarged insulin-stained areas in NPIs ($p < 0.001$,

Fig. 5D). No consistent effect was observed on the NPI intracellular insulin/ATP ratio among the three experiments (Fig. 5A). In addition, under normoxic conditions, we observed a maturation of alpha cells from day 1 to day 9 of culture, as shown by the enlarged glucagon-stained areas ($p < 0.0001$) (Fig. 5E). Low oxygen pressure seemed to hinder this phenomenon, and the O_2 strategy failed to retain alpha cell maturation (Fig. 5E). Altogether, these results underlined the influence of O_2 tension on NPIs maturation and suggested the benefit of the oxygenation strategy to decrease NPIs maturation in BAP after transplantation.

As part of the hypoxia response, we evaluated VEGF release by pancreatic islets in the O_2-balanced BAP or negative and positive controls (Fig. 6A and 6B). As expected, hypoxia enhanced the VEGF/ATP ratio by 132 % ($p < 0.01$) and 192% ($p = 0.0625$) after 3 and 8 days, respectively, compared to the positive control (NPIs cultured under high O_2 tension) (Fig. 6A). At day 3, the hypoxia-driven VEGF production seemed to be prevented by the O_2 balanced BAP ($p = 0.3125$). With more time, however, no significant differences were observed between both conditions despite the oxygen supply (Fig. 6B). In addition, the relative expression of HO-1 in NPIs cultured for 15 days under the different conditions compared to day 1 was quantified to assess islet oxidative stress in response to hypoxia (Fig. 6C). The level of HO-1 mRNA expression in NPIs cultured under high O_2 tension seemed stable from day 1 to day 15, while hypoxia increased HO-1 expression by 1,730%. Despite the benefits previously observed on NPI viability, function, and maturation, the O_2 strategy did not mitigate the effect of hypoxia on HO-1 expression, as similar mRNA levels were observed as in hypoxia.

Discussion

Encapsulation in a biomaterial is essential to isolate transplanted cells from the immune or autoimmune response of the host and allows low or no immunosuppression regimens. However, encapsulation aggravates the O_2 diffusional limitations. Low O_2 tensions of approximately 10 mmHg are encountered in the graft after transplantation during the critical 7 to 14 day period preceding the BAP surface neovascularization[9,13]. This acute hypoxic period is responsible for massive pancreatic islet dysfunction and cell death[8,14]. A diffusion-based device design usually results in an inadequate transplant size with low encapsulated islet density, making it difficult to scale-up BAPs designed for small animals to large animal models or for human recipients[4]. Using the factorial design and RSM methodologies, we designed an O_2-balanced BAP carrying islets at high density under low O_2 tension (10 mm Hg) by incorporating the combination of an O_2 carrier and an *in situ* O_2 generator.

MPIs were used to reduce the animal requirements for the optimization step of our O_2-balanced BAP. The O_2 strategy composed of HEMOXCell and the silicone-CaO_2 disk was efficient to maintain macro-encapsulated MPIs in a viable and functional state. The presence of the O_2 generator showed positive effects on both MPI viability and insulin secretion capacity in a hypoxic environment. On the contrary, the presence of the O_2 generator under normoxic conditions resulted in a slight decrease in the viable cell

content in the BAP. This might be due to the generation of hyperoxic stress within the islets cultured in normoxia with the O_2 generator[37] and/or to the production of toxic reactive oxygen species (ROS) produced by the silicone-CaO_2 disk[24,26,38]. Interestingly, we also highlighted a significant positive effect of the presence of HEMOXCell on the viable cell content in the BAP. Of particular interest, the interaction between HEMOXCell and silicone-CaO_2 showed a positive synergistic effect on the viability of MPI in the BAP. This could be explained by the anti-oxidant properties of the hemoglobin neutralizing the ROS produced by the silicone-CaO_2 disk and by its capacity to increase the O_2 diffusivity in the alginate hydrogel, thereby preventing hyperoxia[24]. Consequently, the best O_2 strategy for the BAP carrying MPIs was the combination of the O_2 carrier and generator.

Using this promising O_2 strategy and the RSM methodology, we designed an O_2 balanced BAP carrying a high density of viable islets for transplantation to sites of low O_2 tension. Islet seeding densities exceeding 300 IEQ/cm^2 *in vitro* decreases cell viability and function, and induces pro-inflammatory responses in human[17] and rat[15] islets. By increasing the O_2 supply to the encapsulated islets with the combination of an O_2 carrier and generator, we increased the pseudo-islet seeding density to 3,284 IEQ/cm^2 in the BAP composed of two 680 µm-thick alginate sheets (21,893 IEQ/mL) cultured in a hypoxic environment (1% O_2). Maintenance of the O_2 balance in the device allowed almost all the seeded MPIs to remain viable over the 24 h culture period. In contrast, the optimal seeding density without silicone-CaO_2 was only 375 IEQ/cm^2. Although the presence of HEMOXCell increased the viability of MPIs in the device, the tested concentrations of hemoglobin did not significantly affect the percentage of viable islets in the BAP. Thus, we selected the highest concentration of hemoglobin assessed to improve O_2 diffusion through the BAP after the O_2 generator was exhausted.

The BAP configuration optimized with the MPI model was extrapolated to BAPs containing primary pancreatic islets isolated from neonate pigs. NPIs remain the most promising alternative to human islets, as pig insulin and metabolic characteristics are very similar to human characteristics[39]. Moreover, naked NPIs exhibit natural resistance to hypoxia in terms of survival and function[20]. The endocrine portion of NPIs is immature and requires a long period before reaching functional maturity[22,40–43]. This maturation process may further be impacted by low O_2 tensions in the graft[44,45]. Placing the presently designed BAP in an environment of low O_2 tension to mimic the O_2 tension in the graft before its vascularization resulted in a significant impairment of the NPIs viability and of their ability to secrete insulin in response to glucose plus theophylline. The discrepancy with previously published results might be explained by the negative effect of the macrocapsule and the high islet density on the O_2 availability in the device versus the use of low-density naked NPIs. Hypoxia also prevented the NPI maturation process observed in the BAP cultured under high O_2 tension, suggesting that the hypoxic environment before graft neovascularization should delay the time needed for NPIs to become functional *in vivo*. Interestingly, our BAP design including the oxygenation system mitigated the adverse effects triggered by hypoxia by improving NPI viability, function, and maturation. Nevertheless, the O_2 strategy failed to prevent NPI

upregulation of mRNA expression of the oxidative stress marker HO-1. This could be linked to the production of ROS by silicone-CaO_2 disk[24,46]. Finally, VEGF was increased in response to hypoxia by NPIs. In the O_2 balanced BAP, this pro-angiogenic response was maintained from days 3 to 8. We[24] and other[30] have already shown that hemoglobin may have a specific proangiogenic effect on pancreatic islets. The Hyperoxic-Hypoxic paradox[47], suggesting that fluctuation in the free O_2 concentration rather than the absolute level of O_2 can be interpreted at the cellular level as a lack of O_2, could also explain the proangiogenic effect triggered by the oxygenation strategy. VEGF secretion could improve BAP engraftment by maintaining a beneficial proangiogenic signal in the absence of O_2 limitation.

The DoE methodology was used to design an O_2 balanced BAP allowing a high islet density by preventing the adverse effect of low O_2 tension encountered in the graft before its vascularization. Use of such an O_2 balanced BAP would lead to an acceptable device size of approximately 180 cm^2 that would carry the 600,000 IEQ needed to achieve normoglycemia in adult human patient[5,19]. Moreover, the total number of islets required to reach therapeutic efficiency in humans might be decreased in this O_2-balanced BAP[4,28,48,49]. In the past, the amount of islets necessary has been defined based on naked pancreatic human islets transplanted into the liver[19]. In this environment, islets are exposed to a hostile microenvironment leading to the rapid death of a large portion of the grafted cells[9,50–52]. By preventing immune reactions and hypoxia-induced damage by encapsulation and adequate O_2 supply, the O_2 balanced BAP could reduce post-transplant cell death and thus the number of pancreatic islets required per human patient. Finally, increasing the O_2 tension in the BAP after transplantation promoted the differentiation and functional maturation of neonate pig islet beta cells in our settings. These results suggest that our oxygenation strategy may improve maturation defects of other promising alternative beta cell sources, such as insulin-producing cells derived from human stem cells[44,53].

Our study has several limitations. Future work must focus on the *in vivo* evaluation of the efficacy of the O_2 balanced BAP in diabetic mice in allo and xenotransplantation model. The use of genetically modified pig knockout for main xenoantigens, such as Neu5Gc and alpha1-3 GAL, could be useful to prevent the specific humoral response[54] and to improve long term engraftment. Another important consideration is the capacity of the O_2 regulated BAP to adapt to the varying O_2 tensions encountered in the transplant site during the graft surface revascularization phase. Indeed, the O_2 tension in the extravascular BAP is expected to rise from 10 mmHg (1% O_2)[10,52] after transplantation to 30 to 40 mmHg (5% O_2) after revascularization of the device[10,11,55,56]. Presently, the O_2 production rate from the silicone-CaO_2 disk was almost constant over 12 days *in vitro*, suggesting that the O_2 balance in the BAP should be maintained during the acute hypoxic period. Thereafter, the O_2 supply from the vasculature may not be sufficient to maintain fully viable and functional cells in the BAP embarking islets at high density. The presence of HEMOXCell could improve the O_2 supply from the graft vascularization during silicone-CaO_2 depletion due to its capacity to potentiate the islet VEGF secretion and to increase O_2 diffusivity through the

alginate hydrogel[24]. Further work is necessary to confirm the stability of HEMOXCell and its capacity to provide sufficient O_2 from the vasculature to maintain the O_2 balance in our high islet density BAP.

Declarations

Acknowledgement. The authors are very grateful to Professor Jun-icho Miyazaki (University Medical School, Osaka, Japan) for the kind gift of the MIN6 cell line. This study was supported by the National Research Agency (ECTIS IHU program, ANR-10-IBHU-005, France), the Pays de la Loire Region (Xenothera program, 2011-12961, France) and the University of Nantes (Interdisciplinary program, 2017-2203).

Author contributions. Conceptualization and Methodology, J-M.B, S.Bekir, A.M. and M.M; Validation, J-M.B, S.Bekir, S.Bosch, D.J, G.M, A.M and M.M; Formal Analysis, S.Bekir, A.M, M.M and P.C, Investigation, M.A, E.B, L.d.B, K.H, S.Bekir, A.M, D.J and M.M; Resources, P.C, D.P, O.G; Writing – Original Draft, J-M. Bach, S.Bekir, A.M. and M.M; Writing – Review & Editing, J-M.B, G.B., S.Bosch, M.M, G.M, D.R. and J-P.S; Visualization, A.M; Supervision, J-M.B and M.M; Funding Acquisition, J-M.B, G.B., D.R., J-P.S; A. M. and S. Bekir should be considered joint first author. J-M. B. and M. M. should be considered joint senior author.

Declaration of interests. The authors declare no competing interests.

Nomenclature. Absorbance unit (AU), adenosine triphosphate (ATP), analysis of variance (ANOVA), bioartificial pancreas (BAP), bovine serum albumin (BSA), design of experiments (DoE), heme oxygenase 1 (HO-1), lactate dehydrogenase (LDH), MIN6 beta cell pseudo-islets (MPIs), neonatal pig islets (NPIs), O_2 consumption rate (OCR), O_2 partial pressure (pO_2), O_2 production rate (OTR), pancreatic progenitor transcription factor (PDX1), peptidylprolyl isomerase A (PPIA), real-time quantitative polymerase chain reactions (RT-qPCR), response surface methodology (RSM), isobutylmethylxanthine (IBMX), islet equivalent quantities (IEQ), relative light units (RLU), reactive oxygen species (ROS), ribosomal protein L19 (RPL19), and vascular endothelial growth factor (VEGF).

References

1. Orive, G. *et al.* Engineering a Clinically Translatable Bioartificial Pancreas to Treat Type I Diabetes. *Trends in Biotechnology* **36**, 445–456 (2018).

2. Klymiuk, N., Ludwig, B., Seissler, J., Reichart, B. & Wolf, E. Current Concepts of Using Pigs as a Source for Beta-Cell Replacement Therapy of Type 1 Diabetes. *Curr Mol Bio Rep* **2**, 73–82 (2016).

3. Colton, C. K. Oxygen supply to encapsulated therapeutic cells. *Adv Drug Deliv Rev* **67–68**, 93–110 (2014).

4. Dulong, J.-L. & Legallais, C. A theoretical study of oxygen transfer including cell necrosis for the design of a bioartificial pancreas. *Biotechnol Bioeng* **96**, 990–998 (2007).

5. Barkai, U., Rotem, A. & de Vos, P. Survival of encapsulated islets: More than a membrane story. *World J Transplant* **6**, 69–90 (2016).

6. Avgoustiniatos, E. S. & Colton, C. K. Effect of external oxygen mass transfer resistances on viability of immunoisolated tissue. *Ann N Y Acad Sci* **831**, 145–167 (1997).

7. Komatsu, H., Kandeel, F. & Mullen, Y. Impact of Oxygen on Pancreatic Islet Survival. *Pancreas* **47**, 533–543 (2018).

8. Moritz, W. *et al.* Apoptosis in hypoxic human pancreatic islets correlates with HIF-1alpha expression. *FASEB J* **16**, 745–747 (2002).

9. Carlsson, P. O., Palm, F., Andersson, A. & Liss, P. Markedly decreased oxygen tension in transplanted rat pancreatic islets irrespective of the implantation site. *Diabetes* **50**, 489–495 (2001).

10. Vériter, S. *et al.* The impact of hyperglycemia and the presence of encapsulated islets on oxygenation within a bioartificial pancreas in the presence of mesenchymal stem cells in a diabetic Wistar rat model. *Biomaterials* **32**, 5945–5956 (2011).

11. Vériter, S. *et al.* Improvement of subcutaneous bioartificial pancreas vascularization and function by coencapsulation of pig islets and mesenchymal stem cells in primates. *Cell Transplant* **23**, 1349–1364 (2014).

12. Iwata, H., Arima, Y. & Tsutsui, Y. Design of Bioartificial Pancreases From the Standpoint of Oxygen Supply. *Artif Organs* **42**, E168–E185 (2018).

13. Jones, G. L. *et al.* Time course and quantification of pancreatic islet revascularization following intraportal transplantation. *Cell Transplant* **16**, 505–516 (2007).

14. Dionne, K. E., Colton, C. K. & Yarmush, M. L. Effect of hypoxia on insulin secretion by isolated rat and canine islets of Langerhans. *Diabetes* **42**, 12–21 (1993).

15. Rodriguez-Brotons, A. *et al.* Impact of Pancreatic Rat Islet Density on Cell Survival during Hypoxia. *J Diabetes Res* **2016**, 3615286 (2016).

16. Paredes-Juarez, G. A. *et al.* DAMP production by human islets under low oxygen and nutrients in the presence or absence of an immunoisolating-capsule and necrostatin-1. *Sci Rep* **5**, 14623 (2015).

17. Brandhorst, D., Brandhorst, H., Mullooly, N., Acreman, S. & Johnson, P. R. V. High Seeding Density Induces Local Hypoxia and Triggers a Proinflammatory Response in Isolated Human Islets. *Cell Transplant* **25**, 1539–1546 (2016).

18. Fisher, R. Johnson, A.S., R.J. Fisher, G.C. Weir and C.K. Colton, “Oxygen Consumption and Diffusion in Assemblages of Respiring Spheres: Performance Enhancement of a Bio-artificial Pancreas”, Chem. Eng.

Sci, Vol.64, No.22, 4470-87, (2009). (2009).

19. Barton, F. B. *et al.* Improvement in outcomes of clinical islet transplantation: 1999-2010. *Diabetes Care* **35**, 1436–1445 (2012).

20. Emamaullee, J. A., Shapiro, A. M. J., Rajotte, R. V., Korbutt, G. & Elliott, J. F. Neonatal porcine islets exhibit natural resistance to hypoxia-induced apoptosis. *Transplantation* **82**, 945–952 (2006).

21. Pepper, A. R. *et al.* A prevascularized subcutaneous device-less site for islet and cellular transplantation. *Nat Biotechnol* **33**, 518–523 (2015).

22. Trivedi, N., Steil, G. M., Colton, C. K., Bonner-Weir, S. & Weir, G. C. Improved vascularization of planar membrane diffusion devices following continuous infusion of vascular endothelial growth factor. *Cell Transplant* **9**, 115–124 (2000).

23. Johnson, A. S. *et al.* Quantitative assessment of islets of Langerhans encapsulated in alginate. *Tissue Eng Part C Methods* **17**, 435–449 (2011).

24. Mouré, A. *et al.* Extracellular hemoglobin combined with an O2-generating material overcomes O2 limitation in the bioartificial pancreas. *Biotechnology and bioengineering* **116**, 1176–1189 (2019).

25. Barkai, U. *et al.* Enhanced oxygen supply improves islet viability in a new bioartificial pancreas. *Cell Transplant* **22**, 1463–1476 (2013).

26. McQuilling, J. P., Sittadjody, S., Pendergraft, S., Farney, A. C. & Opara, E. C. Applications of particulate oxygen-generating substances (POGS) in the bioartificial pancreas. *Biomater Sci* **5**, 2437–2447 (2017).

27. Pedraza, E., Coronel, M. M., Fraker, C. A., Ricordi, C. & Stabler, C. L. Preventing hypoxia-induced cell death in beta cells and islets via hydrolytically activated, oxygen-generating biomaterials. *Proc Natl Acad Sci U S A* **109**, 4245–4250 (2012).

28. Evron, Y. *et al.* Long-term viability and function of transplanted islets macroencapsulated at high density are achieved by enhanced oxygen supply. *Sci Rep* **8**, 6508 (2018).

29. Mandenius, C.-F. & Brundin, A. Bioprocess optimization using design-of-experiments methodology. *Biotechnology Progress* **24**, 1191–1203 (2008).

30. Rodriguez-Brotons, A. *et al.* Comparison of Perfluorodecalin and HEMOXCell as Oxygen Carriers for Islet Oxygenation in an In Vitro Model of Encapsulation. *Tissue Eng Part A* **22**, 1327–1336 (2016).

31. Le Pape, F. *et al.* HEMOXCell, a New Oxygen Carrier Usable as an Additive for Mesenchymal Stem Cell Culture in Platelet Lysate-Supplemented Media. *Artif Organs* **41**, 359–371 (2017).

32. Graham, M. L., Bellin, M. D., Papas, K. K., Hering, B. J. & Schuurman, H.-J. Species incompatibilities in the pig-to-macaque islet xenotransplant model affect transplant outcome: a comparison with

allotransplantation. *Xenotransplantation* **18**, 328–342 (2011).

33. Mueller, K. R. *et al.* Differences in glucose-stimulated insulin secretion in vitro of islets from human, nonhuman primate, and porcine origin. *Xenotransplantation* **20**, 75–81 (2013).

34. Papas, K. K. *et al.* Human islet oxygen consumption rate and DNA measurements predict diabetes reversal in nude mice. *Am J Transplant* **7**, 707–713 (2007).

35. Sweet, I. R. *et al.* Glucose-stimulated increment in oxygen consumption rate as a standardized test of human islet quality. *Am J Transplant* **8**, 183–192 (2008).

36. Kitzmann, J. P. *et al.* Real-time assessment of encapsulated neonatal porcine islets prior to clinical xenotransplantation. *Xenotransplantation* **19**, 333–336 (2012).

37. Ma, Z., Moruzzi, N., Catrina, S.-B., Grill, V. & Björklund, A. Hyperoxia inhibits glucose-induced insulin secretion and mitochondrial metabolism in rat pancreatic islets. *Biochem Biophys Res Commun* **443**, 223–228 (2014).

38. Forget, A. *et al.* Oxygen-Releasing Coatings for Improved Tissue Preservation. *ACS Biomater. Sci. Eng.* **3**, 2384–2390 (2017).

39. Samy, K. P., Martin, B. M., Turgeon, N. A. & Kirk, A. D. Islet cell xenotransplantation: a serious look toward the clinic. *Xenotransplantation* **21**, 221–229 (2014).

40. De Mesmaeker, I. *et al.* Increase Functional β-Cell Mass in Subcutaneous Alginate Capsules With Porcine Prenatal Islet Cells but Loss With Human Adult Islet Cells. *Diabetes* **67**, 2640–2649 (2018).

41. Kin, T. & Korbutt, G. S. Delayed functional maturation of neonatal porcine islets in recipients under strict glycemic control. *Xenotransplantation* **14**, 333–338 (2007).

42. Li, W.-C. *et al.* Porcine Neonatal Pancreatic Cell Clusters Maintain Their Multipotency in Culture and After Transplantation. *Sci Rep* **8**, 8212 (2018).

43. Omer, A. *et al.* Survival and maturation of microencapsulated porcine neonatal pancreatic cell clusters transplanted into immunocompetent diabetic mice. *Diabetes* **52**, 69–75 (2003).

44. Hakim, F. *et al.* High oxygen condition facilitates the differentiation of mouse and human pluripotent stem cells into pancreatic progenitors and insulin-producing cells. *J Biol Chem* **289**, 9623–9638 (2014).

45. Heinis, M. *et al.* Oxygen tension regulates pancreatic beta-cell differentiation through hypoxia-inducible factor 1alpha. *Diabetes* **59**, 662–669 (2010).

46. Coronel, M. M., Geusz, R. & Stabler, C. L. Mitigating hypoxic stress on pancreatic islets via in situ oxygen generating biomaterial. *Biomaterials* **129**, 139–151 (2017).

47. Hadanny, A. & Efrati, S. The Hyperoxic-Hypoxic Paradox. *Biomolecules* **10**, (2020).

48. Sörenby, A. K. *et al.* Preimplantation of an immunoprotective device can lower the curative dose of islets to that of free islet transplantation: studies in a rodent model. *Transplantation* **86**, 364–366 (2008).

49. Mitchelson, F., Safley, S. A., Gordon, K., Weber, C. J. & Sambanis, A. Peritoneal dissolved oxygen and function of encapsulated adult porcine islets transplanted in streptozotocin diabetic mice. *Xenotransplantation* e12673 (2021) doi:10.1111/xen.12673.

50. Davalli, A. M. *et al.* Vulnerability of islets in the immediate posttransplantation period. Dynamic changes in structure and function. *Diabetes* **45**, 1161–1167 (1996).

51. Emamaullee, J. A. & Shapiro, A. M. J. Factors Influencing the Loss of β-Cell Mass in Islet Transplantation. *Cell Transplant* **16**, 1–8 (2007).

52. Mattsson, G., Jansson, L. & Carlsson, P.-O. Decreased vascular density in mouse pancreatic islets after transplantation. *Diabetes* **51**, 1362–1366 (2002).

53. Cechin, S. *et al.* Influence of in vitro and in vivo oxygen modulation on β cell differentiation from human embryonic stem cells. *Stem Cells Transl Med* **3**, 277–289 (2014).

54. Salama, A. *et al.* Neu5Gc and α1-3 GAL xenoantigen knockout does not affect glycemia homeostasis and insulin secretion in pigs. *Diabetes* **66**, 987–993 (2017).

55. Manavella, D. D. *et al.* Two-step transplantation with adipose tissue-derived stem cells increases follicle survival by enhancing vascularization in xenografted frozen-thawed human ovarian tissue. *Hum Reprod* **33**, 1107–1116 (2018).

56. Van Eyck, A.-S. *et al.* Electron paramagnetic resonance as a tool to evaluate human ovarian tissue reoxygenation after xenografting. *Fertil Steril* **92**, 374–381 (2009).

57. Korbutt, G. S. *et al.* Large scale isolation, growth, and function of porcine neonatal islet cells. *J Clin Invest* **97**, 2119–2129 (1996).

58. Miyazaki, J. *et al.* Establishment of a pancreatic beta cell line that retains glucose-inducible insulin secretion: special reference to expression of glucose transporter isoforms. *Endocrinology* **127**, 126–132 (1990).

59. Ricordi, C. *et al.* Islet isolation assessment in man and large animals. *Acta Diabetol Lat* **27**, 185–195 (1990).

Figures

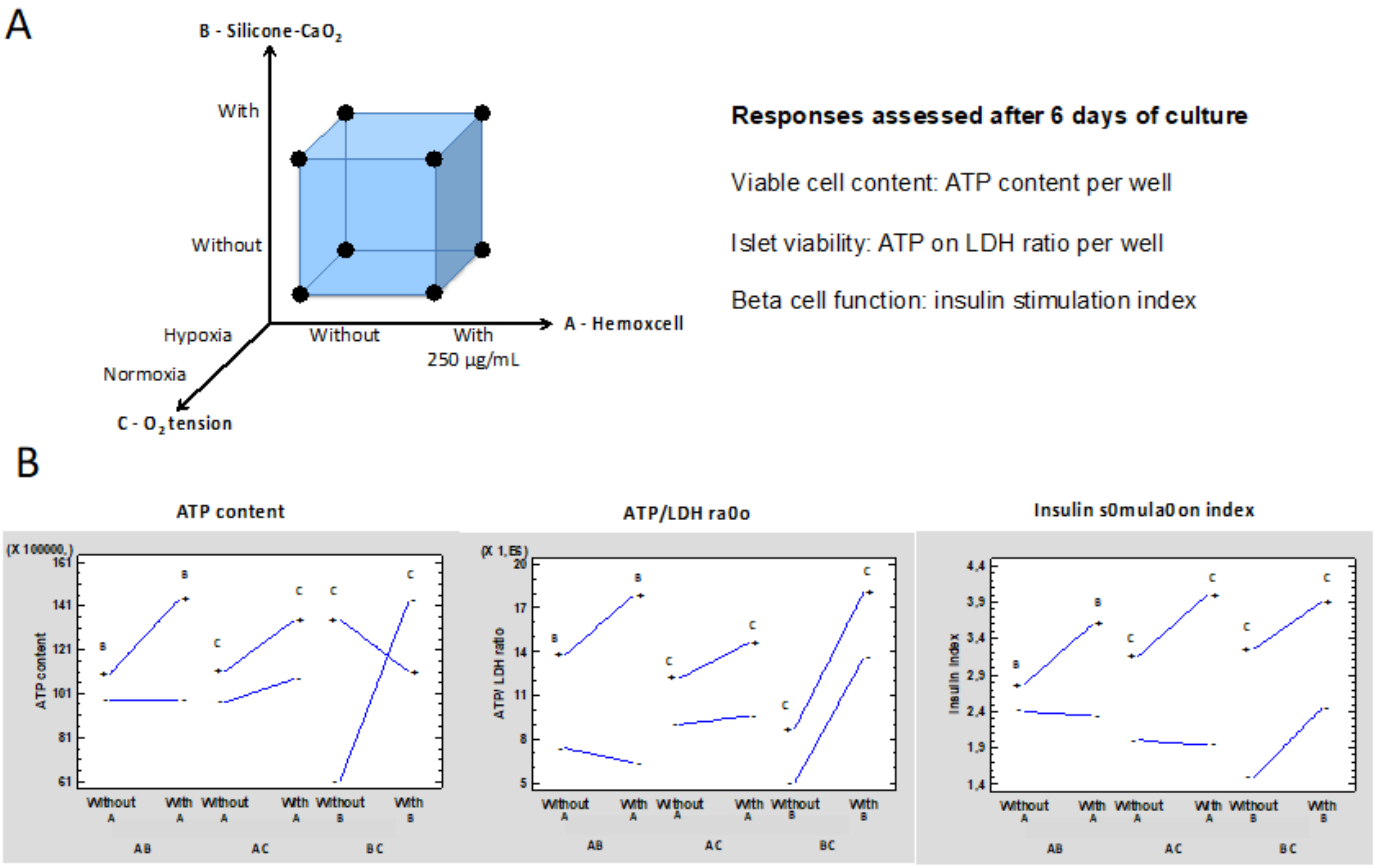

Figure 1

Screening experimental design. (A) The screening of the oxygenation strategies was done on MPIs encapsulated in alginate macrobeads using a full factorial design 23. The three factors studied and their levels were: without/with HEMOXCell, without/with silicone-CaO2, and normoxic/hypoxic O2 tension. The response variables assessed after 6 days of culture were the intracellular ATP content per well (RLU), ATP/LDH viability ratio per well (RLU/ AU), and the insulin stimulation index. (B) Interaction plots of the screening DoE. Interactions involving AB HEMOXCell/silicone-CaO2, AC HEMOXCell/O2 tension, and BC silicone-CaO2/O2 tension are displayed concerning ATP content, ATP/LDH ratio, and insulin stimulation index.

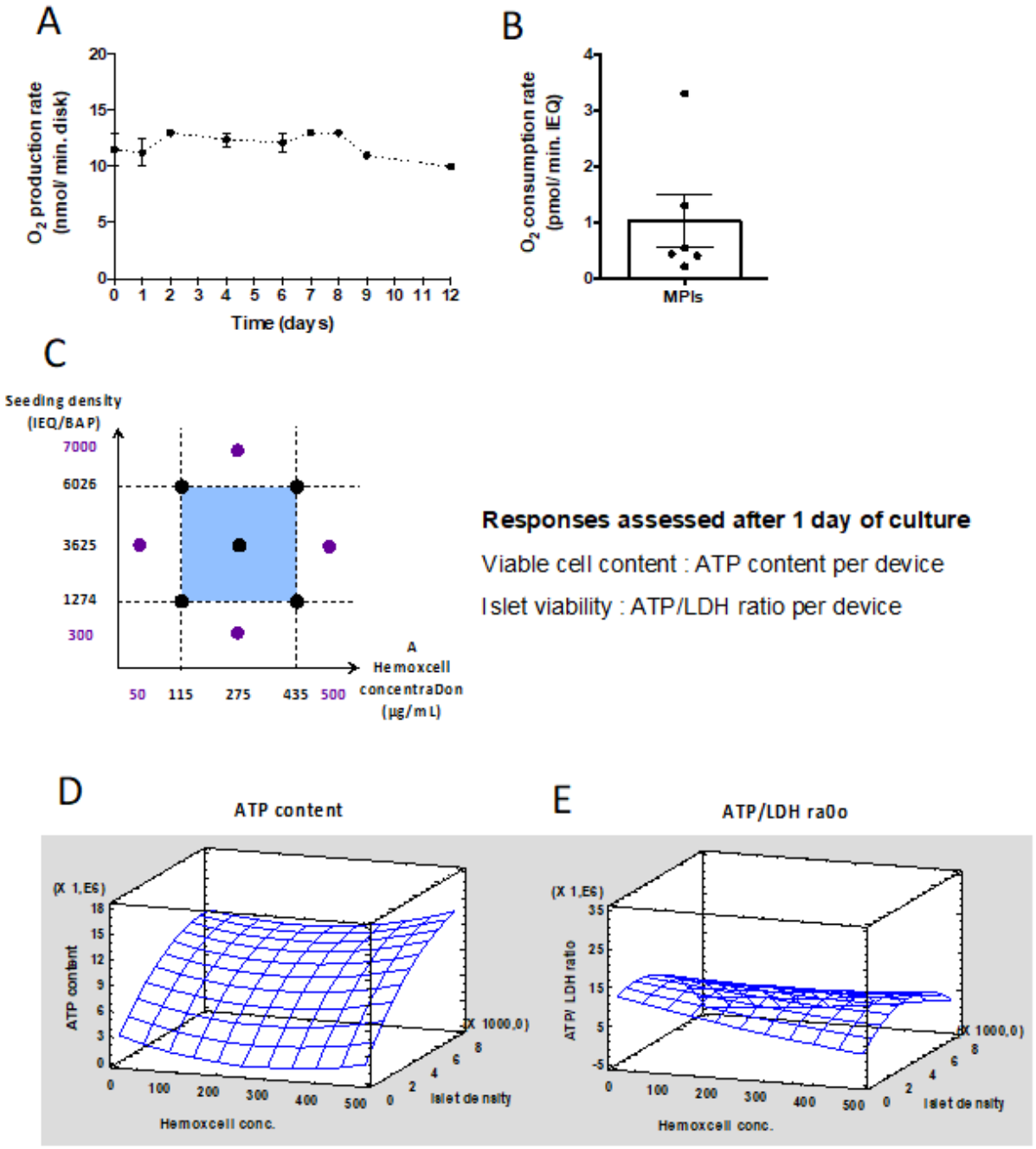

Figure 2

Optimization experimental design. Based on the silicone-CaO2 O2 production rate (A) and the pseudo-islet O2 consumption rate (B), a central composite design was used to optimize the HEMOXCelll concentration and islet seeding density in the BAP (C). The response variables, intracellular ATP content (RLU), and ATP/LDH viability ratio (RLU/AU) per device were assessed for MPIs encapsulated in alginate sheets after 1 day of culture. Results of O2 production rate (n=2) and consumption rate (n=6) are presented as mean ± SEM of independent experiments. (D, E) Response surface analysis for the optimization DoE. The plots represent the effects of the HEMOXCell concentration, islet seeding density,

and their interaction on the ATP content (D) and the ATP/LDH ratio (E) in the BAP after 1 day of culture under low O2 tension.

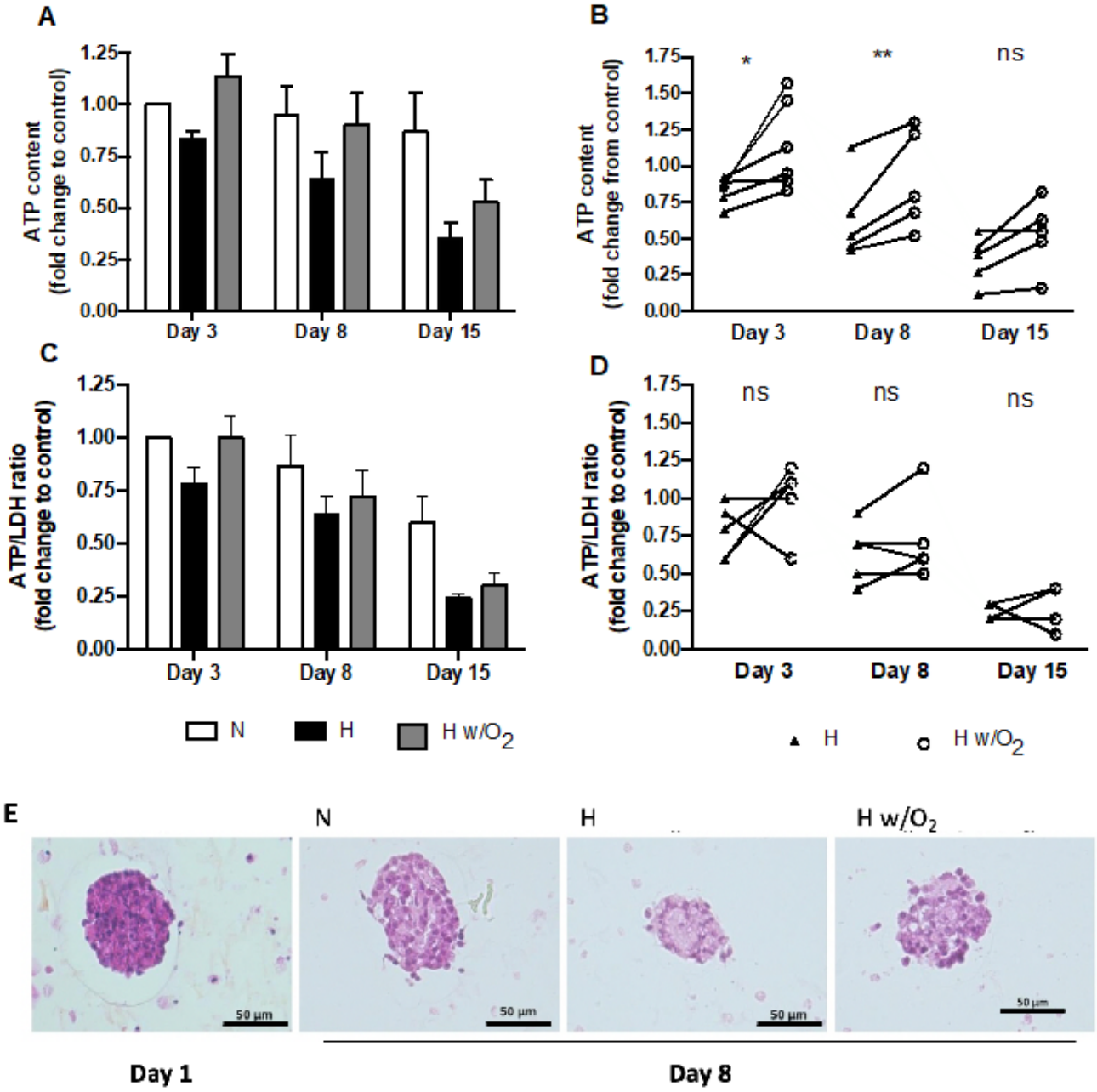

Figure 3

Viability of neonate pig islets embarked in O2-balanced BAP. Alginate encapsulated NPIs (3,000 IEQ/150 µL) were cultured for 3, 8 and 15 days under normoxic condition (N, 20% O2, positive control, white bar) or hypoxic condition (1% O2) without O2 strategy (H, negative control, black bar and closed triangle) or with O2-strategy composed of silicone-CaO2 disk and 500 µg/mL HEMOXCell by alginate (H with O2, O2 balanced BAP, grey bars and open circle). Fold change in (A, B) total metabolic activity (ATP content, RLU) and in (C, D) viability (ATP/LDH ratio, RLU/AU) of encapsulated NPIs compared to the control cultured at day 3 under normoxia without O2 strategy. Results from independent experiments (n=4–6) are expressed

(A, C) as mean percentage ± SEM or (B, D) individual results matched in hypoxia with or without O2 strategy. *p<0.05, **p<0.01, ns : non-significant (Non-parametric Wilcoxon apparatus test). (E) Histological analyzes of formalin-fixed paraffin-embedded NPIs 4 µm thick cross-sections stained with hematoxylin-eosin-saffron on pre-encapsulated NPIs, 24 h after isolation (day 1) and on decapsulated NPIs after 8 days of culture within the BAPs.

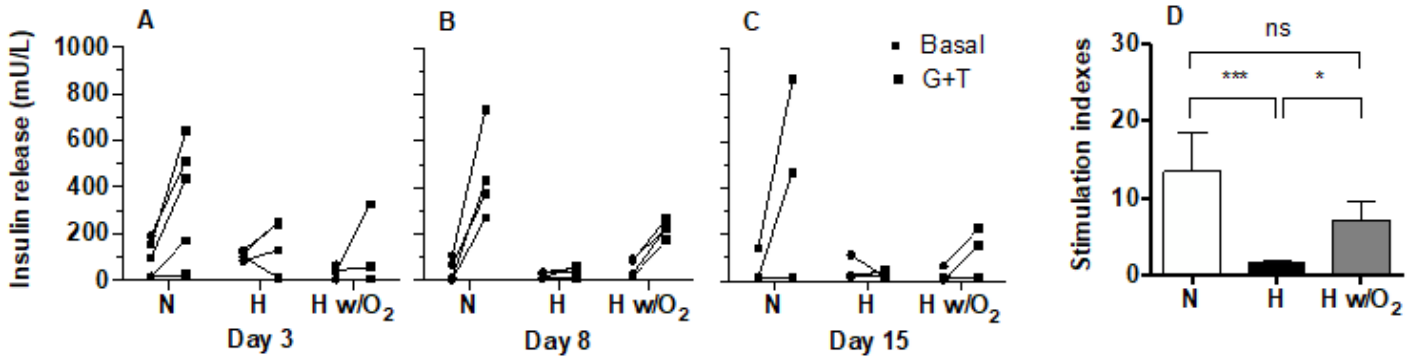

Figure 4

Function of neonate pig islets (NPIs) in O2 balanced BAPs. Alginate encapsulated NPIs (3000 IEQ/150 µL) were cultured for 3, 8, and 15 days under normoxic (N, 20% O2, positive control, white bar) or hypoxic (1% O2, negative control) conditions without the O2 strategy (H, back bar), or with the O2 strategy composed of silicone-CaO2 disk and 500 µg/mL HEMOXCell by alginate (H with O2, O2 balanced BAP, grey bars). (A, B, C) Glucose plus theophylline (G + T) responsive insulin release by 30 min sequential incubations of alginate encapsulated NPIs in basal medium (closed circle) and glucose plus theophylline stimulation (closed square) after 3 (A), 8 (B) and 15 (C) days of culture. (D) Stimulation indexes (ratio of high glucose plus theophylline stimulation over basal insulin secretion) of alginate encapsulated NPIs after 3, 8, and 15 days of culture. Results from independent experiments (n=4–6) are expressed (D) as mean percentage ± SEM or (A, B, C) individual results matched in basal or stimulation media. * p <0.05, ***p<0.005, ns : non-significant (Non-parametric Wilcoxon or Mann-Whitney test).

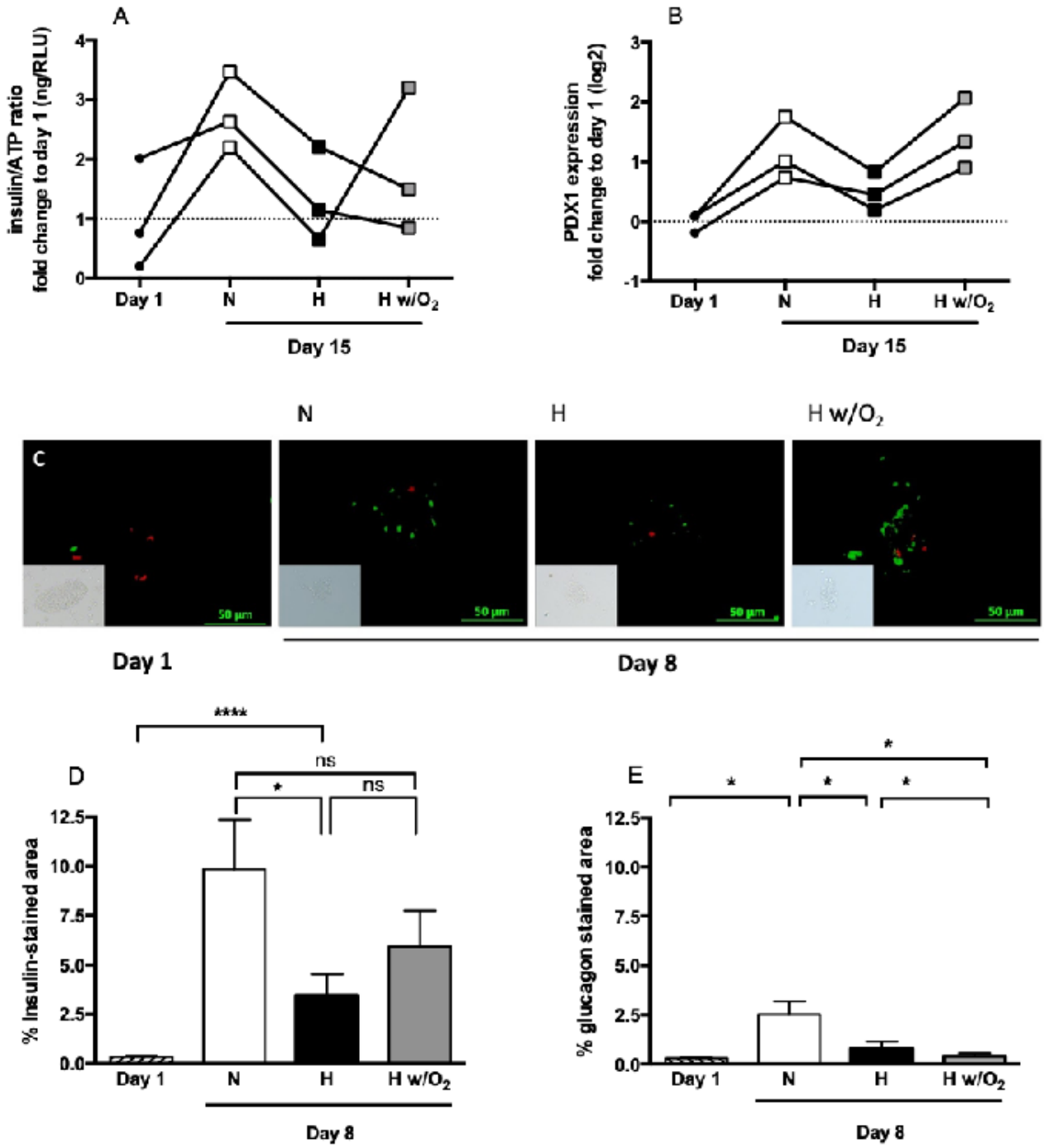

Figure 5

Effect of O2 strategy on the maturation of neonate pig islets (NPIs) embarked in O2 balanced BAPs. The analyses were performed on pre-encapsulated NPIs 24 h after isolation (day 1) and on encapsulated NPIs cultured for 8 or 15 days within BAPs in normoxic (20% O2, N, positive control) and hypoxic (1% O2, negative control) conditions without the O2 strategy (H) or with the O2 strategy composed of silicone-CaO2 disk and 500 µg/mL HEMOXCell by alginate (H with O2) (n=3–4 pigs). (A) Intracellular insulin by ATP content ratio. (B) Relative quantitative RT-PCR expression analysis of pancreatic progenitor transcription factor (PDX1). (C) Immunostaining of insulin ß cells (green, Alexa-Fluor 488) and glucagon

α cells (red, Alexa-Fluor 555) staining of NPIs in 4 µm thick cross-sections. Views in white light are shown to the lower-left of each photo. The scale is indicated in each picture. (D) Percentage of mean insulin-positive area per islet. (E) Percentage of mean glucagon-positive area per islet. The percentages of insulin and glucagon were quantified within 150 islets in day 1 (n = 4 pigs) and an average of 30 islets per condition after day 8 of culture (n=3 pigs). * p <0.05, ****p<0.0005, ns : non-significant (Unpaired parametric t-test)

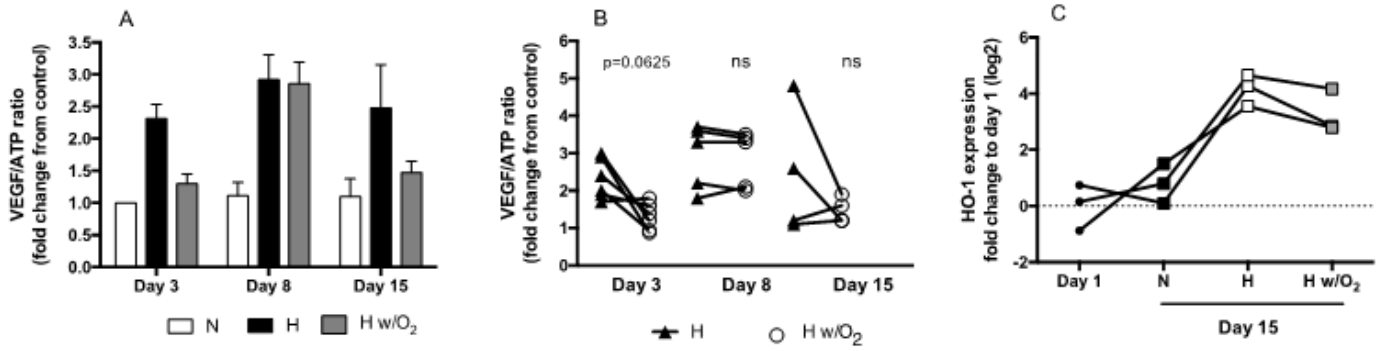

Figure 6

Hypoxic signature of neonate pig islets (NPIs) in O2 balanced BAPs. Alginate encapsulated NPIs (3000 IEQ/150 µL) were cultured for 3, 8, and 15 days under normoxic (N, 20% O2, positive control, white bar) or hypoxic (1% O2, negative control) condition without O2 strategy (H, back bar) or with O2 strategy composed of silicone-CaO2 disk and 500 µg/mL HEMOXCell by alginate (H with O2, O2-balanced BAP, grey bars). Fold change in VEGF secretion by total metabolic activity (AU/RLU) of encapsulated NPIs compared to the control cultured for 3 days under normoxia without O2 strategy. Results from independent experiments (n=4–6) are expressed (A) as mean percentage ± SEM or (B) individual results matched in hypoxia with or without O2-strategy. ns : non-significant (Non-parametric Wilcoxon apparatus test). (C) Relative quantitative RT-PCR expression analysis of Heme oxygenase (HO-1) of decapsulated NPIs cultured for 15 days within BAPs (n=3).

Supplementary Files

This is a list of supplementary files associated with this preprint. Click to download.

- Supplementaryforreview.docx